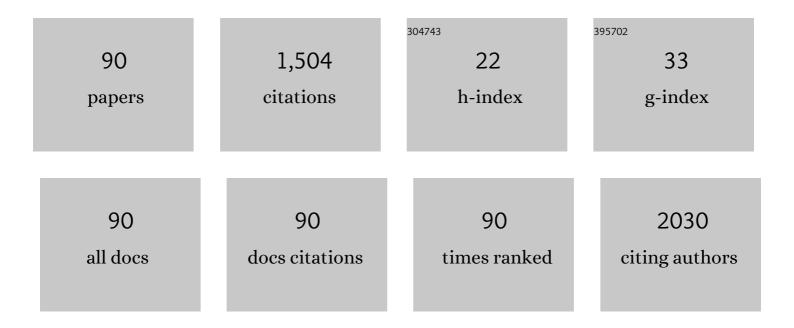
List of Publications by Year in descending order

Source: https://exaly.com/author-pdf/2006390/publications.pdf Version: 2024-02-01



#	Article	IF	CITATIONS
1	ZnO-NWs/Cu-based metallic glass nanotube array (ZNWs/Cu-MeNTA) for field emission properties. Journal of Alloys and Compounds, 2022, 890, 161846.	5.5	4
2	Surface modified highly porous egg-shell membrane derived granular activated carbon coated on paper substrate and its humidity sensing properties. Materials Chemistry and Physics, 2022, 277, 125486.	4.0	6
3	Surface and interface properties of monolayer graphene on hydrophobic and hydrophilic ultrananocrystalline diamond structures for hydrogen sensing applications. International Journal of Hydrogen Energy, 2022, 47, 4959-4969.	7.1	2
4	Structure dependence of gas sensing responsivity on graphene nanoribbons covered TiO2 nanotubes, nano-bugles array. Journal of Materials Science: Materials in Electronics, 2022, 33, 6082.	2.2	1
5	Reducing noise current in exfoliated WS ₂ nanosheets using an ultra-nanocrystalline diamond substrate and their enhanced NIR photodetection properties. Journal of Materials Chemistry C, 2022, 10, 6061-6069.	5.5	1
6	Effect of MoS2 solution on reducing the wall thickness of ZnO nanotubes to enhance their hydrogen gas sensing properties. Journal of Alloys and Compounds, 2021, 854, 157102.	5.5	14
7	Boron-doped graphene from boron-doped copper substrate for self-powered photodetector. Materials Science and Engineering B: Solid-State Materials for Advanced Technology, 2021, 263, 114814.	3.5	1
8	ZnO-NWs/metallic glass nanotube hybrid arrays: Fabrication and material characterization. Surface and Coatings Technology, 2021, 408, 126785.	4.8	12
9	Crystalline Nanodiamond-Induced Formation of Carbon Nanotubes for Stable Hydrogen Sensing. ACS Applied Nano Materials, 2021, 4, 2840-2848.	5.0	9
10	Cesium tungsten bronze nanostructures and their highly enhanced hydrogen gas sensing properties at room temperature. International Journal of Hydrogen Energy, 2021, 46, 25752-25762.	7.1	18
11	Modified interfaces of twisted root-like 2D configured ZnO hierarchical nanostructures through surface lattice coating of NiO/graphene and their enhanced UV photodetection properties. Journal of Alloys and Compounds, 2021, 868, 159240.	5.5	10
12	Role of Nanodiamond Grains in the Exfoliation of WS ₂ Nanosheets and Their Enhanced Hydrogen-Sensing Properties. ACS Applied Materials & Interfaces, 2021, 13, 48260-48269.	8.0	5
13	Reversibly photoswitchable gratings prepared from azobenzene-modified tethered poly(methacrylic) Tj ETQq1 1	0.784314 7.8	rgBT /Overl
14	Enhancement of UV Photodetection Properties of Hierarchical Core–Shell Heterostructures of a Natural Sericin Biopolymer with the Addition of ZnO Fabricated on Ultra-Nanocrystalline Diamond Layers. ACS Applied Materials & Interfaces, 2020, 12, 3254-3264.	8.0	5
15	Structural Engineering of Dispersed Graphene Flakes into ZnO Nanotubes on Discontinues Ultraâ€Nanocrystalline Diamond Substrates for Highâ€Performance Photodetector with Excellent UV Light to Dark Current Ratios. Advanced Materials Interfaces, 2020, 7, 1901694.	3.7	7
16	Exfoliated MoSe ₂ Nanosheets Doped on the Surface of ZnO Nanorods for Hydrogen Sensing Applications. ACS Applied Nano Materials, 2020, 3, 12139-12147.	5.0	24
17	Superficial Edge Effect of N ₂ -Doped Nanodiamond on the Highly Stable Nonenzymatic Glucose Detection Properties of Dispersed Graphene Flakes/Ni Nanostructures. ACS Applied Bio Materials, 2020, 3, 5966-5973.	4.6	5
18	Self-growth of graphene nanosheets on a crystalline nanodiamond substrate using NixZnxO catalyst and their efficient photodetection properties. Applied Materials Today, 2020, 20, 100679.	4.3	1

#	Article	IF	CITATIONS
19	Effect of PMMA on the surface of exfoliated MoS2 nanosheets and their highly enhanced ammonia gas sensing properties at room temperature. Journal of Alloys and Compounds, 2020, 832, 155005.	5.5	24
20	Highâ€Performance Sensor Based on Thinâ€Film Metallic Glass/Ultraâ€nanocrystalline Diamond/ZnO Nanorod Heterostructures for Detection of Hydrogen Gas at Room Temperature. Chemistry - A European Journal, 2019, 25, 10385-10393.	3.3	22
21	Interface engineering of ultrananocrystalline diamond/MoS2-ZnO heterostructures and its highly enhanced hydrogen gas sensing properties. Sensors and Actuators B: Chemical, 2019, 292, 70-79.	7.8	48
22	Improving the optical and crystal properties of ZnO nanotubes via a metallic glass quantum dot underlayer. Journal of Materials Chemistry C, 2019, 7, 5163-5171.	5.5	1
23	Silicon- and oxygen-codoped graphene from polycarbosilane and its application in graphene/n-type silicon photodetectors. Applied Surface Science, 2019, 464, 125-130.	6.1	14
24	Highly enhanced hydrogen sensing properties of sericin-induced exfoliated MoS2 nanosheets at room temperature. Sensors and Actuators B: Chemical, 2019, 279, 138-147.	7.8	46
25	Concurrent enhancement in the H ₂ and UV sensing properties of ZnO nanostructures through discontinuous lattice coating of La ³⁺ <i>via</i> partial p–n junction formation. Journal of Materials Chemistry C, 2018, 6, 2387-2395.	5.5	17
26	The Significant Role of Hydrophilic and Hydrophobic Interfaces in Grapheneâ€Based 1D Heterostructures for Highly Enhanced Electron Emission. Advanced Materials Interfaces, 2018, 5, 1701148.	3.7	2
27	Interfacial Effect of Oxygen-Doped Nanodiamond on CuO and Micropyramidal Silicon Heterostructures for Efficient Nonenzymatic Glucose Sensor. ACS Applied Bio Materials, 2018, 1, 1579-1586.	4.6	24
28	Role of conductive nitrogen incorporated diamond nanowires for enhancing the UV detection and field emission properties of ZnO nanotubes. Materials and Design, 2018, 154, 130-139.	7.0	14
29	Bioâ€industrial Waste Silk Fibroin Protein and Carbon Nanotubeâ€Induced Carbonized Growth of Oneâ€Dimensional ZnOâ€based Bioâ€nanosheets and their Enhanced Optoelectronic Properties. Chemistry - A European Journal, 2018, 24, 12574-12583.	3.3	8
30	Antigen detection with thermosensitive hydrophilicity of poly(<i>N</i> -isopropylacrylamide)-grafted poly(vinyl chloride) fibrous mats. Journal of Materials Chemistry B, 2018, 6, 3486-3496.	5.8	9
31	Hierarchical morphology and hydrogen sensing properties of N2-based nanodiamond materials produced through CH4/H2/Ar plasma treatment. Applied Surface Science, 2018, 457, 367-375.	6.1	13
32	High-Performance Electron Field Emitters and Microplasma Cathodes Based on Conductive Hybrid Granular Structured Diamond Materials. ACS Applied Materials & Interfaces, 2017, 9, 4916-4925.	8.0	12
33	Multifunctional sustainable materials: the role of carbon existing protein in the enhanced gas and UV sensing performances of ZnO-based biofilms. Journal of Materials Chemistry C, 2017, 5, 5239-5247.	5.5	29
34	Core-Shell P-N Junction Si Nanowires as Rapid Response and High-Sensitivity pH Sensor. IEEE Sensors Journal, 2017, 17, 3967-3974.	4.7	7
35	Simple Synthesis of Eco-Friendly Multifunctional Silk-Sericin Capped Zinc Oxide Nanorods and Their Potential for Fabrication of Hydrogen Sensors and UV Photodetectors. ACS Sustainable Chemistry and Engineering, 2017, 5, 4002-4010.	6.7	18
36	Self-Assembled Hierarchical Interfaces of ZnO Nanotubes/Graphene Heterostructures for Efficient Room Temperature Hydrogen Sensors. ACS Applied Materials & Interfaces, 2017, 9, 12064-12072.	8.0	53

#	Article	IF	CITATIONS
37	Pillar arrays of tethered polyvinyltetrazole on silicon as a visualization platform for sensing of lead ions. Sensors and Actuators B: Chemical, 2017, 243, 234-243.	7.8	25
38	Natural Biowaste-Cocoon-Derived Granular Activated Carbon-Coated ZnO Nanorods: A Simple Route To Synthesizing a Core–Shell Structure and Its Highly Enhanced UV and Hydrogen Sensing Properties. ACS Applied Materials & Interfaces, 2017, 9, 39771-39780.	8.0	33
39	Few-Layer Thin-Film Metallic Glass-Enhanced Optical Properties of ZnO Nanostructures. ACS Applied Materials & Interfaces, 2017, 9, 39475-39483.	8.0	18
40	Functionalization of CVD Grown Graphene with Downstream Oxygen Plasma Treatment for Glucose Sensors. Journal of the Electrochemical Society, 2017, 164, B336-B341.	2.9	25
41	Interfacial effects in ZnO nanotubes/needle-structured graphitic diamond nanohybrid for detecting dissolved acetone at room temperature. Applied Surface Science, 2017, 426, 630-638.	6.1	3
42	Phosphor-Free InGaN White Light Emitting Diodes Using Flip-Chip Technology. Materials, 2017, 10, 432.	2.9	9
43	Investigation of Rapid Low-Power Microwave-Induction Heating Scheme on the Cross-Linking Process of the Poly(4-vinylphenol) for the Gate Insulator of Pentacene-Based Thin-Film Transistors. Materials, 2017, 10, 742.	2.9	1
44	Effects of the F4TCNQ-Doped Pentacene Interlayers on Performance Improvement of Top-Contact Pentacene-Based Organic Thin-Film Transistors. Materials, 2016, 9, 46.	2.9	12
45	Real-Time Packing Behavior of Core-Shell Silica@Poly(N-isopropylacrylamide) Microspheres as Photonic Crystals for Visualizing in Thermal Sensing. Polymers, 2016, 8, 428.	4.5	10
46	Nitrogen Incorporated Ultrananocrystalline Diamond Microstructures From Biasâ€Enhanced Microwave N ₂ /CH ₄ â€Plasma Chemical Vapor Deposition. Plasma Processes and Polymers, 2016, 13, 419-428.	3.0	15
47	Poly(4-vinylphenol) gate insulator with cross-linking using a rapid low-power microwave induction heating scheme for organic thin-film-transistors. APL Materials, 2016, 4, 036105.	5.1	14
48	Engineered design and fabrication of long lifetime multifunctional devices based on electrically conductive diamond ultrananowire multifinger integrated cathodes. Journal of Materials Chemistry C, 2016, 4, 9727-9737.	5.5	5
49	Highly sensitive pH dependent acetone sensor based on ultrananocrystalline diamond materials at room temperature. RSC Advances, 2016, 6, 102821-102830.	3.6	3
50	Improvement in reliability of amorphous indium–gallium–zinc oxide thin-film transistors with Teflon/SiO ₂ bilayer passivation under gate bias stress. Japanese Journal of Applied Physics, 2016, 55, 02BC17.	1.5	8
51	Structure and field emission of graphene layers on top of silicon nanowire arrays. Applied Surface Science, 2016, 362, 250-256.	6.1	14
52	Enhancement of plasma illumination characteristics via typical engineering of diamond–graphite nanocomposite films. CrystEngComm, 2016, 18, 1800-1808.	2.6	1
53	Novel LTPS-TFT Pixel Circuit with OLED Luminance Compensation for 3D AMOLED Displays. Journal of Display Technology, 2016, 12, 425-428.	1.2	40
54	Fast Photoresponse and Long Lifetime UV Photodetectors and Field Emitters Based on ZnO/Ultrananocrystalline Diamond Films. Chemistry - A European Journal, 2015, 21, 16017-16026.	3.3	23

#	Article	IF	CITATIONS
55	Heterogranular-Structured Diamond–Gold Nanohybrids: A New Long-Life Electronic Display Cathode. ACS Applied Materials & Interfaces, 2015, 7, 27078-27086.	8.0	15
56	Highly Conductive Diamond–Graphite Nanohybrid Films with Enhanced Electron Field Emission and Microplasma Illumination Properties. ACS Applied Materials & Interfaces, 2015, 7, 14035-14042.	8.0	13
57	Bifunctional superparamagnetic–luminescent core–shell–satellite structured microspheres: preparation, characterization, and magnetodisplay application. Journal of Materials Chemistry C, 2015, 3, 4603-4615.	5.5	22
58	WO3/TiO2 core–shell nanostructure for high performance energy-saving smart windows. Solar Energy Materials and Solar Cells, 2015, 133, 32-38.	6.2	35
59	Color-tunable mixed photoluminescence emission from Alq3 organic layer in metal-Alq3-metal surface plasmon structure. Nanoscale Research Letters, 2014, 9, 569.	5.7	7
60	Improvement in Brightness Uniformity by Compensating for the Threshold Voltages of Both the Driving Thin-Film Transistor and the Organic Light-Emitting Diode for Active-Matrix Organic Light-Emitting Diode Displays. International Journal of Photoenergy, 2014, 2014, 1-8.	2.5	2
61	Effect of gas enhanced metal-semiconductor-metal UV photodetectors based on thermal annealing tungsten oxide thin film prepared by sol–gel method. Journal of Materials Science: Materials in Electronics, 2014, 25, 408-413.	2.2	7
62	Poole-Frenkel effect on electrical characterization of Al-doped ZnO films deposited on p-type GaN. Journal of Applied Physics, 2014, 115, 113705.	2.5	12
63	Hybrid structure of graphene sheets/ZnO nanorods for enhancing electron field emission properties. Applied Surface Science, 2014, 289, 384-387.	6.1	25
64	Bias-Enhanced Nucleation and Growth Processes for Ultrananocrystalline Diamond Films in Ar/CH ₄ Plasma and Their Enhanced Plasma Illumination Properties. ACS Applied Materials & Interfaces, 2014, 6, 10566-10575.	8.0	26
65	Hydrogen-sensing response of grass-like carbon nanotube/nickel nanostructure by microwave treatment. Carbon, 2014, 76, 410-416.	10.3	8
66	Aggregated TiO2 nanotubes with high field emission properties. Applied Surface Science, 2014, 311, 339-343.	6.1	12
67	ZnO Branched Nanowires and the p-CuO/n-ZnO Heterojunction Nanostructured Photodetector. IEEE Nanotechnology Magazine, 2013, 12, 263-269.	2.0	62
68	Temperature effect on hydrogen response for cracked carbon nanotube/nickel (CNT/Ni) composite film with horizontally aligned carbon nanotubes. Sensors and Actuators B: Chemical, 2013, 185, 548-552.	7.8	14
69	ZnO/Silicon Nanowire Hybrids Extended-Gate Field-Effect Transistors as pH Sensors. Journal of the Electrochemical Society, 2013, 160, B78-B82.	2.9	25
70	Low temperature synthesis of ZnO nanotubes based hydrogen sensors. , 2013, , .		1
71	Key technique for texturing a uniform pyramid structure with a layer of silicon nitride on monocrystalline silicon wafer. Applied Surface Science, 2013, 266, 245-249.	6.1	20
72	A facile synthesis of ZnO nanotubes and their hydrogen sensing properties. Applied Surface Science, 2013, 280, 945-949.	6.1	45

BOHR-RAN HUANG

#	Article	IF	CITATIONS
73	Bilayer Structure of ZnO Nanorod/Nanodiamond Film Based Ultraviolet Photodetectors. Journal of the Electrochemical Society, 2013, 160, H509-H512.	2.9	18
74	Field emission properties of zinc oxide/zinc tungstate (ZnO/ZnWO 4) composite nanorods. Surface and Coatings Technology, 2013, 231, 289-292.	4.8	16
75	Rice-straw-like structure of silicon nanowire arrays for a hydrogen gas sensor. Nanotechnology, 2013, 24, 475502.	2.6	24
76	Core-Shell Structure of a Silicon Nanorod/Carbon Nanotube Field Emission Cathode. Journal of Nanomaterials, 2012, 2012, 1-6.	2.7	4
77	Low-Frequency Noise Characteristics of GaN Schottky Barrier Photodetectors Prepared With Nickel Annealing. IEEE Sensors Journal, 2012, 12, 2824-2829.	4.7	10
78	Core–shell structure of zinc oxide/indium oxide nanorod based hydrogen sensors. Sensors and Actuators B: Chemical, 2012, 174, 389-393.	7.8	58
79	CuO Nanowire-Based Humidity Sensor. IEEE Sensors Journal, 2012, 12, 1884-1888.	4.7	44
80	Long-term stability of a horizontally-aligned carbon nanotube field emission cathode coated with a metallic glass thin film. Carbon, 2012, 50, 1619-1624.	10.3	16
81	Palladium nanoparticles modified carbon nanotube/nickel composite rods (Pd/CNT/Ni) for hydrogen sensing. Sensors and Actuators B: Chemical, 2012, 162, 108-113.	7.8	49
82	Gas Ionization Sensors with Carbon Nanotube/Nickel Field Emitters. Journal of Nanoscience and Nanotechnology, 2011, 11, 10849-10853.	0.9	0
83	A novel technique to fabricate horizontally aligned CNT nanostructure film for hydrogen gas sensing. International Journal of Hydrogen Energy, 2011, 36, 15919-15926.	7.1	10
84	Improvement of n-ZnO/p-Si photodiodes by embedding of silver nanoparticles. Journal of Nanoparticle Research, 2011, 13, 4757-4763.	1.9	12
85	The Effect of Tetrafluoromethane Plasma Post-Treatment on the Electrical Property of Tungsten Oxide Nanowires. Journal of Nanoscience and Nanotechnology, 2011, 11, 7693-7699.	0.9	3
86	Leaf-like carbon nanotube/nickel composite membrane extended-gate field-effect transistors as <i>p</i> H sensor. Applied Physics Letters, 2011, 99, .	3.3	20
87	Effect of rapid thermal annealing treatment on the field-emission characteristics of nanocrystalline diamonds grown on various metal/silicon substrates. Journal of Materials Science: Materials in Electronics, 2010, 21, 385-392.	2.2	1
88	Effect of XeF laser treatment on structure of nanocrystalline diamond films. Diamond and Related Materials, 2010, 19, 445-448.	3.9	7
89	Field Emission and Electric Discharge of Nanocrystalline Diamond Films. Journal of Electronic Materials, 2009, 38, 750-755.	2.2	4
90	Highly Sensitive ZnO Nanowire Acetone Vapor Sensor With Au Adsorption. IEEE Nanotechnology Magazine, 2008, 7, 754-759.	2.0	95